Environment International 201 (2025) 109553

Contents lists available at ScienceDirect

Environment International

journal homepage: www.elsevier.com/locate/envint

Full length article

Transformation metabolites of phthalate esters (PAEs) inhibited rice growth through jasmonic acid signaling pathway

Yingying Sun [a,b,1], Jie Chen [a,b,c,1], Wei Wang [a,b,c], Lizhong Zhu [a,b,c,*]

[a] College of Environmental and Resource Sciences, Zhejiang University, Hangzhou, Zhejiang 310058, China
[b] Zhejiang Provincial Key Laboratory of Organic Pollution Process and Control, Hangzhou, Zhejiang 310058, China
[c] Ministry of Education Key Laboratory of Environment Remediation and Ecological Health, Zhejiang University, Hangzhou, Zhejiang 310058, China

ARTICLE INFO

Handling Editor: Adrian Covaci

Keywords:
Phthalate esters
Transformation products
Jasmonic acid signaling pathway
Pest defense
Growth inhibition

ABSTRACT

Phthalate esters (PAEs) were ubiquitous in agricultural soils and could be metabolized after being absorbed by crops, posing significant implications for crop yield and quality. We hypothesize that monophthalates (mPAEs), the hydrolyzed products of PAEs, might mimic phytohormone jasmonic acid (JA) to activate the JA signaling pathway, therefore enhancing the defense towards pests and inhibiting the rice plant growth. Taking dibutyl phthalate (DBP) as a representative PAE, our study discovered that DBP exposure significantly induced JA-related outcomes including decreased larval weight (9.58–18.8%), and rice biomass (11.7–34.2%). Under the conditions where the JA content remained unchanged, monobutyl phthalate (MBP), the hydrolyzed product of DBP, triggered the JA signaling pathway, evidenced by significantly upregulated genes encoding coronatine insensitive 1 (COI1) (1.56–1.73 fold), jasmonate ZIM-domain (JAZ) (4.33–7.71 fold), MYC2 transcription factor (2.07–2.87 fold), and promoted phytoalexins production in downstream signaling. MBP conjugated with isoleucine, and the conjugate subsequently mimicked a JA bioactivator (JA-isoleucine conjugate) to occupy the binding site of COI1-JAZ co-receptor protein, thereby initiating the JA signaling pathway. These JA-related outcomes and mechanism were consistently evidenced in rice exposed to other four typical PAEs, and the aliphatic chain length of selected PAEs indicated a negative contribution to these observations. In this study, we discovered a unconventional mechanism through which the transformation metabolites of PAEs elicit pest defense while simultaneously inhibiting rice growth, providing insights into the risk assessment of PAEs on crop yields and quality.

1. Introduction

Phthalates (PAEs), the esters of phthalic acid, were extensively utilized as plasticizers in agriculture, industry, and household products, to improve the processability and flexibility (Nguyen et al., 2022a; Wang and Kannan, 2023; Weng et al., 2023). PAEs exhibited a significant risk of leaking into the environment, leading to their prevalent occurrence across air, water, and soil (Shi et al., 2012; Net et al., 2015; Dueñas-Moreno et al., 2022; Henkel et al., 2022; Shinohara et al., 2024). In particular, the widespread and continued application of agricultural plastic films led to high residue of PAEs in agricultural soils, ranging from μg/kg to mg/kg (Guo et al., 2021; Wang et al., 2021; Zhang et al., 2021). Collective studies reported that several commonly used PAEs were frequently detected in the agricultural soils in China with the mean concentration reaching up to 24.0 mg/kg (Wu et al., 2015), which was over 100 times higher than that of the detected organochlorine pesticides (mean value of 197 μg/kg) (Zhou et al., 2013). A field survey conducted in the Shandong Peninsula, East China, on 36 vegetable fields with plastic film mulching revealed that PAEs were universally detected in all sampled soils and the concentrations ranging from 1.37 to 18.81 mg/kg (average value of 6.47 mg/kg), with dibutyl phthalate (DBP) as the predominant PAE congener (Li et al., 2016). Previous field investigations demonstrated that PAEs, for example, DBP, could be uptaken by rice plants with the levels of 0.03–26.27 mg/kg (Sun et al., 2015; Cheng et al., 2020; Cheng et al., 2021), and further hydrolyzed to monophthalates (mPAEs), which were the primary transformation products. It was reported that up to 41.7 % of DBP was transformed to monobutyl phthalate (MBP) in rice seedlings after 192-hour exposure

* Corresponding author at: College of Environmental and Resource Sciences, Zhejiang University, Hangzhou, Zhejiang 310058, China.
E-mail address: zlz@zju.edu.cn (L. Zhu).
[1] Y. Y. Sun and J. Chen contributed equally.

https://doi.org/10.1016/j.envint.2025.109553
Received 11 November 2024; Received in revised form 24 April 2025; Accepted 23 May 2025
Available online 27 May 2025

(Zhu et al., 2019). Current studies have massively compared the adverse effects of both parent compounds and metabolic products of PAEs on plants (Gao et al., 2017; Gao et al., 2021; Jiang et al., 2022). Notably, the mPAEs appear to exert greater toxicities than their parent compounds (Kratochvil et al., 2019; Ma et al., 2020; Jiao et al., 2020). However, the underlying mechanisms responsible for the heightened toxicity of mPAEs was not uncovered in plants.

Intriguingly, mPAEs, featuring aliphatic chains and acetate side chains, were structurally similar to phytohormone jasmonic acid (JA). JA signaling pathway, as a dedicated mechanism for pest defense, plays an essential role for plants in sensing and response to herbivore attacks by transcriptional regulation and metabolic reprogramming (Li et al., 2002). It enhanced plant tolerance towards insects by producing phytotoxins, which reconfigured the availability of carbon in plants skewing from growth-related processes to defense-related processes, ultimately resulting in growth suppression (Guo et al., 2018; Li et al., 2022; Nguyen et al., 2022b). For example, jasmonates mobilize carbon availability-mediated growth-defense trade-offs after the leaf-herbivore attack in *Nicotiana attenuata*. It enhanced pest resistance through the biosynthesis of specialized metabolites such as phenylpropanoids and terpenoids, whereas inhibited plant growth by reducing sugar and starch contents (Machado et al., 2013). The application of an exogenous JA activator was also capable of diminishing growth and enhancing pest resistance by activating the JA signaling pathway (Fu et al., 2021). We proposed that mPAEs, as JA structural analogues, may activate the JA signaling pathway, switching on pest defense response at the cost of plant growth.

Several key proteins determined the activation of JA signaling transduction, including JA-amido synthetase (JAR1), coronatine insensitive 1 (COI1), jasmonate ZIM-domain (JAZ), and MYC2 transcription factor (Fig. S1) (Thines et al., 2007; Zander et al., 2020). In normal conditions, JA and its bioactive form jasmonoyl–isoleucine (JA-Ile) was typically at a low level, and Jasmonate ZIM-domain (JAZ) protein physically binds to MYC2 transcription factor, thus inhibiting the JA-response genes. When suffering from pest attack, JA was immediately synthesized and coupled with isoleucine (Ile) to form the JA-Ile conjugate, with the assistance of JAR1 (Howe et al., 2018). The JA-Ile conjugate was perceived by the protein complex COI1-JAZ, thereby releasing the MYC2 transcription factor and permitting the expression of JA-responsive genes, i.e., the biosynthesis of pest-toxic compounds like diterpenoids and flavonoids (Chen et al., 2024). Consequently, the defensive processes against pests were enhanced and the growth of vegetative tissues was inhibited (Fu et al., 2021). The perception and binding of JA-Ile to the COI1-JAZ co-receptor complex was frequently considered as a molecular switch step for the initiation of the JA signal pathway (Montea et al., 2022). The aliphatic chain and the other side chain containing isoleucine of JA-Ile, which were fully accommodated in the binding pocket, achieved the interaction of JA-Ile and COI1-JAZ co-receptor (Sheard et al., 2010). We proposed that the metabolic products of DBP (MBP-Ile) might interact with the COI1-JAZ receptors, initiating the JA signaling pathway to enhance pest defense and hinder plant growth.

In this study, rice (*Oryza sativa* L.), serving as a staple food for nearly half of the global population, was employed as the plant model (Deng et al., 2019; Kah et al., 2019). DBP, prevalent in both the aquatic environment and agricultural soils, was employed as the representative PAE (Niu et al., 2014; Lee et al., 2019; Liang et al., 2024). The objectives of this study included: (i) to explore the growth inhibition in DBP-exposed rice plants; (ii) to analyze the roles of DBP and its transformation products in JA signaling pathway using RNA transcriptome analysis and UPLC-QTOF-MS; and (iii) to determine the interaction of the transformation products of DBP and COI1-JAZ co-receptor complex. Furthermore, other four PAEs, including dimethyl phthalate (DMP), diethyl phthalate (DEP), dioctyl phthalate (DnOP), and bis(2-ethylhexyl) phthalate (DEHP), were included to validate the role of mPAEs as JA structural analogues. The findings of this study facilitate our understanding of the environmental risks and the mechanism of PAEs and their transformation products in plants.

2. Materials and methods

2.1. Chemicals

Standard chemicals of DBP (CAS No. 84-74-2), MBP (CAS No. 131-70-4), DMP (CAS No. 131-11-3), DEP (CAS No. 84-66-2), DnOP (CAS No. 117-84-0), and DEHP (CAS No. 117-81-7) were purchased from Aladdin (Shanghai, China). JA was purchased from Rhawn (Shanghai, China). Detailed information was presented in Table S1. Organic reagents used in this study, including methanol, acetone, dichloromethane, and hexane, were of analytical or HPLC grade.

2.2. Rice cultivation and exposure experiments

Seeds of rice (*Oryza sativa* L., Lianjing-7 cultivar) were acquired from Zhejiang Academy of Agricultural Sciences (Hangzhou, China). After disinfecting with 3 % (v/v) H_2O_2 for 30 min and rinsing with deionized water several times, the plump seeds were immersed with deionized water for 48 h in the dark. Rice seeds were cultured in Hoagland nutrient solution (pH 5.8) for 8 days in a plant chamber at 25 °C, 70 % relative humidity, 14 h/10 h light/dark cycle, and light intensity of 250 μmol/(photons m^2 s). Selecting twenty seedlings with the same growth conditions as one group and was transferred into brown glass jars containing 480 mL Hoagland nutrient solution. DBP was dissolved in acetone as a stock solution, and the exposure concentrations were set at 0.2, 0.4, 0.8, 1.8, and 3.6 μM, based on the actual environmental concentration (Le et al., 2021). JA treatments (20 μM) was also cultivated as positive controls to compare the effects of MBP and JA directly. In the experimental design, < 0.05 % (v/v) acetone was incorporated into both the treatment group and the solvent control group to eliminate potential solvent interference. This ensures that observed differences between groups could be exclusively attributed to DBP rather than acetone effects. After exposure in a plant chamber for 14 days, rice seedlings were harvested for biological analyses. The detection methods and and quality control and quality assurance (QA/QC) were shown in Text S1 and Text S2 (Cheng et al., 2021). The concentrations of DBP and MBP in rice seedlings were shown in Table S3.

2.3. Detection of growth indicators

Fresh rice seedlings were rinsed thoroughly with deionized water and dried with absorbent paper. Rice lengths were measured with a straightedge. 10 rice seedlings were selected for weighing the biomass. Rice root morphology was scanned using an EPSON Expression (EPSON Perfection V800, Hangzhou, China) and analyzed detailed parameters by WinRHIZO (WR, Canada Reagent Instruments). The contents of starch were measured following the manufacturers' protocol of the total starch assay kit (Beijing Solarbio Technology Co., Ltd, China). Detailed information was provided in Text S3.

2.4. Transcriptome analysis of rice leaves

Total RNA was extracted from rice seedlings using TRIzol reagent according to the manufacturer's instructions (Magen) and was detected based on the A260/A280 absorbance ratio using a Nanodrop ND-2000 system (Thermo Scientific, USA). Paired-end libraries were prepared using an ABclonal mRNA-seq Lib Prep Kit (ABclonal, China) following the manufacturer's instructions. The sequencing library was constructed using the Illumina-HiSeq platform (Agilent, USA) with the assistance of Shanghai Applied Protein Technology Co., Ltd. (Shanghai, China). Differentially expressed genes (DEGs) with adjusted p-value < 0.05 and $|\log_2(\text{Fold Change, FC})| \geq 1$ were considered to be significant. The Gene Ontology (GO), Kyoto Encyclopedia of Genes and Genomes (KEGG), and protein–protein interaction (PPI) network analysis were performed to

identify the significantly altered pathways and explore the interrelationship of DEGs and their expression. The detailed information was shown in Text S4.

2.5. Quantitative real-time fluorescence polymerase chain reaction

Total RNA was extracted from rice seedlings using a plant total RNA extraction kit (Tiangen Biotech, Beijing, China), and NanoDrop-2000 (Wilmington, USA) was used to determine the concentration and quality of RNA. Subsequently, the RNA was reversed into cDNA by FastKing reverse transcription kit (Tiangen Biotech, Beijing, China). SuperReal PreMix Color kit (Tiangen Biotech, Beijing, China) was used for qRT-PCR according to the manufacturer's instructions and run in StepOnePlus real-time PCR system (Applied Biosystems, USA) to collect the fluorescence signal. Relative gene expression levels were determined according to the $2^{-\Delta\Delta Ct}$ method and normalized by each reference gene as a quantitative control. The PCR primers of cDNA sequences of target genes were designed using Primer-BLAST of NCBI (https://www.ncbi.nlm.nih.gov/tools/primer-blast) and shown in Table S4.

2.6. Detection of phytoalexins, jasmonic acid (JA), and JA-isoleucine

The content of phytoalexins (e.g., momilactones, phytocassanes, and oryzalexins), JA, and JA-isoleucine was determined following the manufacturers' protocols of ELISA kits (Jiangsu meimian Biotechnology Co. Ltd, China). The detailed procedures were provided in Text S5 and Text S6.

2.7. Evaluation of rice resistance to the insect Cnaphalocrocis medinalis

Following a two-week incubation of rice seedlings in nutrient solution containing DBP at concentrations of 0.2, 0.4, 0.8, 1.8, and 3.6 μM. To maintain consistency in the condition of the rice leaves provided to *Cnaphalocrocis medinalis* (rice leaf folder), a new batch was cultivated every two days. The rice leaves were subsequently cut into 8 cm sections and placed in petri dishes with perforated lids, sealed with gauze to allow air exchange and also prevent escape of the larvae. Then, five uniformly grown first instar larvae of *Cnaphalocrocis medinalis* were selected and introduced into each dish. These dishes were then kept in an artificial climatic chamber set to maintain a stable environment of 25 °C temperature, 70 % relative humidity, and 14 h-light /10 h-dark cycle. The leaves within the dishes were treated with a preservative solution twice daily, once in the morning and once in the evening. The leaves were also replaced every three days to ensure freshness and adequate nutrition for the larvae. The larvae were weighed on the 7th and 14th days, allowing assessment of growth and health impacts due to exposure to DBP through the treated leaves. Twenty replicates were set for each treatment.

2.8. Detection of transformation products by UPLC-QTOF-MS

The transformation products of DBP were detected using the method described by Xing et al. with minor modifications (Xing et al., 2023). In brief, freeze-dried rice seedlings were ground into powder and weighed 500 mg. Subsequently, 10 mL of acetonitrile (containing 2 % formic acid) was added, followed by an ultrasonication for 30 min. The supernatant of thrice repreated extraction was combined. N-propyl ethylenediamine/silica composite cartridges were used for sample purification. After concentration under a nitrogen stream, the samples were reconstituted using 1 mL of methanol and filtered with 0.22 μm PTFE filters. Transformation products of DBP were then analyzed using ultraperformance liquid chromatography (Waters Corp., Milford, MA, USA) coupled to a quadrupole time-of-flight mass spectrometry (QTOF MS; SCIEXTripleTOF 5600plus system, SCIEX, Framingham, USA) equipped with an ACQUITY UPLC BEH C18 column (2.1 × 100 mm, 1.7 μm, Waters, USA), in the positive ionization (ESI^+) mode. A full scan was performed within the mass-to-charge ratio (m/z) range of 100–2000 for precursor ions and 50–500 for product ions. The information-dependent acquisition (IDA) method was used to identify DBP metabolites and eliminate background interference. Data were analyzed utilizing the PeakView software (SCIEX). Detailed instrumental parameters were provided in Text S7. Molecular weight error, i.e., the discrepancy between theoretical and measured molecular weights, was less than 10 ppm.

2.9. Homology modeling and molecular docking

The 3-D structure of COI1-JAZ co-receptor complexes of rice was constructed by the homology modeling method (https://www.rcsb.org/pdb/). The homology modeling was performed by Discovery Studio 2019 software, and detailed information was provided in Text S7. Ramachandran plot was used to assess the model reliability, as shown in Fig. S8. Molecular docking simulations were carried out by Discovery Studio 2019. Prior to docking, ligand binding sites of COI1-JAZ co-receptor complexes were marked via site finding tools, which began from the common region of COI1 and the Jas motif of JAZ (JAZ degron). The docking operation was performed using the CDOCKER method, setting the COI1-JAZ co-receptor to be rigid and allowing complete flexibility for tiny molecules. CHARMM force field was used to find the possible binding sites. The highest scoring (i.e., lowest docking energy) docked model of a molecule was chosen from the docking data to represent the most advantageous binding mode.

2.10. Statistical analysis

All biological treatments were repeated at least triplicates. Data were analyzed by One-way analysis of variance (ANOVA) to compare statistical differences using IBM SPSS 25.0 and mean ± standard deviation (SD) were expressed in the graph. The statistical significance ''*'' and ''**'' were accepted at a level of $p < 0.05$ and $p < 0.01$, respectively. Data was visualized using Origin 2021. Linear correlation relationship was analyzed between binding affinity and JA signaling pathway.

3. Results and discussion

3.1. Plant growth under DBP stress

The activation of the JA signaling pathway typically induced growth inhibition (Huot et al., 2014; Takaoka et al., 2018). Thus, growth parameters including rice biomass and shoot length, as well as root length, weight, and surface area were quantified. A decreased growth of the rice exposed to DBP was observed in this study. Specifically, the biomass of rice seedlings exhibited no significant changes at 0.2, 0.4, and 0.8 μM of DBP, but was notably reduced by 11.7–34.2 % at 1.8 and 3.6 μM ($p < 0.05$) (Fig. 1a). Besides, the length, weight, and surface area of the roots were significantly diminished by 11.0–24.0 %, 8.6–23.6 %, and 25.0–52.3 %, respectively (Fig. 1 and Fig. S2). The inhibition of plant growth under DBP stress was also observed in previous study (Xing et al., 2023). Making up 38 % of plant dry matter, carbohydrates were the cornerstone of the structure construction in plants. Starch, as a crucial component of carbohydrates, particularly provides the necessary energy and carbon sources for plant development (Bertoft, 2017). In this study, starch content was continuously decreased by 13.8–47.0 % in a dose-dependent manner from 0.2 to 3.6 μM DBP ($p < 0.05$) (Fig. 1d). The decline in prior to the observable growth inhibition, especially at minimal concentrations, hints at significant disruptions in the metabolic network of rice and might be linked to the stress defense. Understanding its dual role in disrupting plant defense-growth trade-offs is critical for ecological risk assessment.

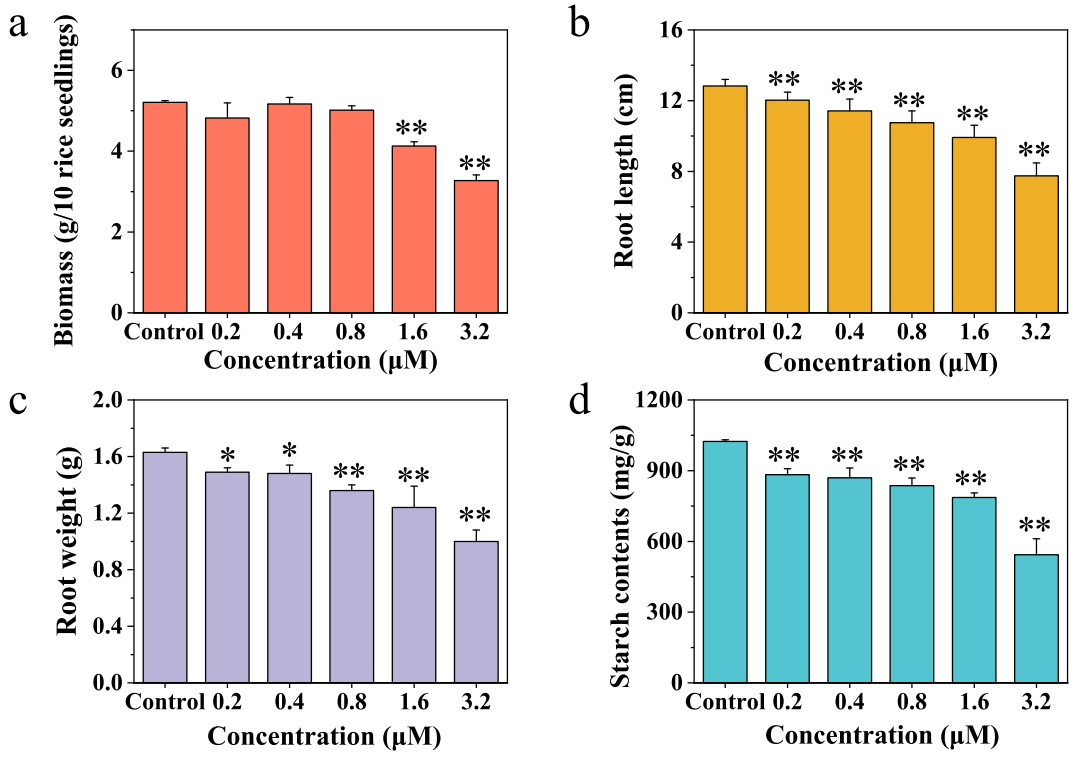

Fig. 1. Changes of rice biomass (a), root length (b), root weight (c), and starch contents (d). These parameters were evaluated with triplicates. The asterisks * and ** represent statistically significant difference at levels of $p < 0.05$ and $p < 0.01$, respectively.

3.2. The activation of JA signaling pathway under DBP exposure

To explore the underlying mechanism of the observed abnormal physiological status under DBP exposure, the transcriptome was utilized to investigate the global response in rice leaves subjected to DBP stress. Principal component analysis (PCA) clearly differentiated the DBP-treated group from the controls, revealing a substantial alteration in the rice transcriptome profiles due to DBP exposure (Fig. S3a). In total, 3624 and 2382 genes were found to be upregulated and downregulated, respectively after being treated with DBP (Fig. S3b). Gene Ontology (GO) annotation of these differentially expressed genes (DEGs) predominantly classified these DEGs into biological processes, highlighting the involvement in various metabolic and biosynthetic pathways such as "response to chemical", "secondary metabolite biosynthetic process," "diterpenoid metabolic process," and "phenylpropanoid biosynthetic process" (Fig. S3c). These compounds were downstream products of the JA signaling pathway and were critical to pest defense in plants. The Kyoto Encyclopedia of Genes and Genomes (KEGG) pathway analysis further aligned with these insights (Fig. 2a), and protein–protein interaction network analysis also found the JA signaling pathway regulates those aforementioned DEGs related to biotic resistance responses (Fig. 2b). These results underscored that the perturbation of JA signaling pathway was likely to be a specific mechanism of the response of rice plants towards DBP stress.

An increase in JA and JA-Ile levels was typically essential for activating the JA signaling pathway (Staswick and Tiryaki, 2004; Howe et al., 2018; Li et al., 2020). Specifically, JA was converted to JA bioactive form (i.e., JA-Ile) with the assistance of JAR1, which was further bound to the COI1-JAZ co-receptor and releases MYC2 transcription factor to initiate the signal transduction (Montea et al., 2022; Chen et al., 2024). Interestingly, the contents of JA, JA-Ile, and the transcription levels of JAR1 in rice leaves treated with DBP were not significantly changed under DBP stress (Fig. 2c, d, and Fig. S4). While the genes encoding COI1, JAZ, and MYC2 were significantly upregulated 1.56–1.73 fold, 4.33–7.71 fold, and 2.07–2.87 fold, respectively (Fig. 2e), indicating a significant activation of JA signaling pathway. As the downstream genes (e.g., responsible for the phytoalexins biosynthesis) regulated by the JA signaling pathway, the copalyl diphosphate synthase family (e.g., CPS2 and CPS4) and the kaurene synthase-like family (e.g., KSL4, KSL7, and KSL10), were significantly upregulated by 1.36–3.89 fold and 1.34–7.12 fold, respectively, under DBP exposure (Fig. 2g and Fig. S5). Diterpenoid phytoalexins including momilactones, phytocassanes, and oryzalexins were typical phytoalexins regulated by JA signaling pathway, which protects plants from herbivorous attack by depleting their growth resources (Sun et al., 2023; Wang et al., 2023; Wang et al., 2022), therefore elevated phytoalexins was a metabolic response regulated by JA signaling pathway. The levels of phytoalexin including momilactones, phytocassanes, and oryzalexins in rice leaves were increased by 5.4–19.7 %, 5.3–34.6 %, and 15.0–33.2 %, respectively, under DBP exposure (Fig. 2f). To auxiliarily validate the enhanced resistance of rice against herbivores, we next assessed the weight changes of *Cnaphalocrocis medinalis*, a common rice leaf folder, after consuming DBP-contaminated rice leaves (Zhuang et al., 2021). While their initial weight showed no significant difference on the 7th day, a substantial decrease of 9.58–18.8 % was observed after 14 days' exposure (Fig. S6). While the observed larval weight reduction may appear quantitatively modest, it serves as a direct physiological indicator of JA-mediated pest resistance activation in rice under DBP exposure. This growth reduction reflected the inevitable metabolic trade-off involving significant starch depletion (Machado et al., 2013; Fu et al., 2021), which may translate to important long-term agronomic consequences, particularly regarding reproductive development and grain-filling efficiency of rice plants. In summary, these evidences suggested an unusual activation of the JA signaling pathway, which inducing defense-growth trade-offs in rice leaves under DBP exposure. As a xenobiotic chemical, how DBP exposure activate the JA signaling pathway independent of JA is elusive.

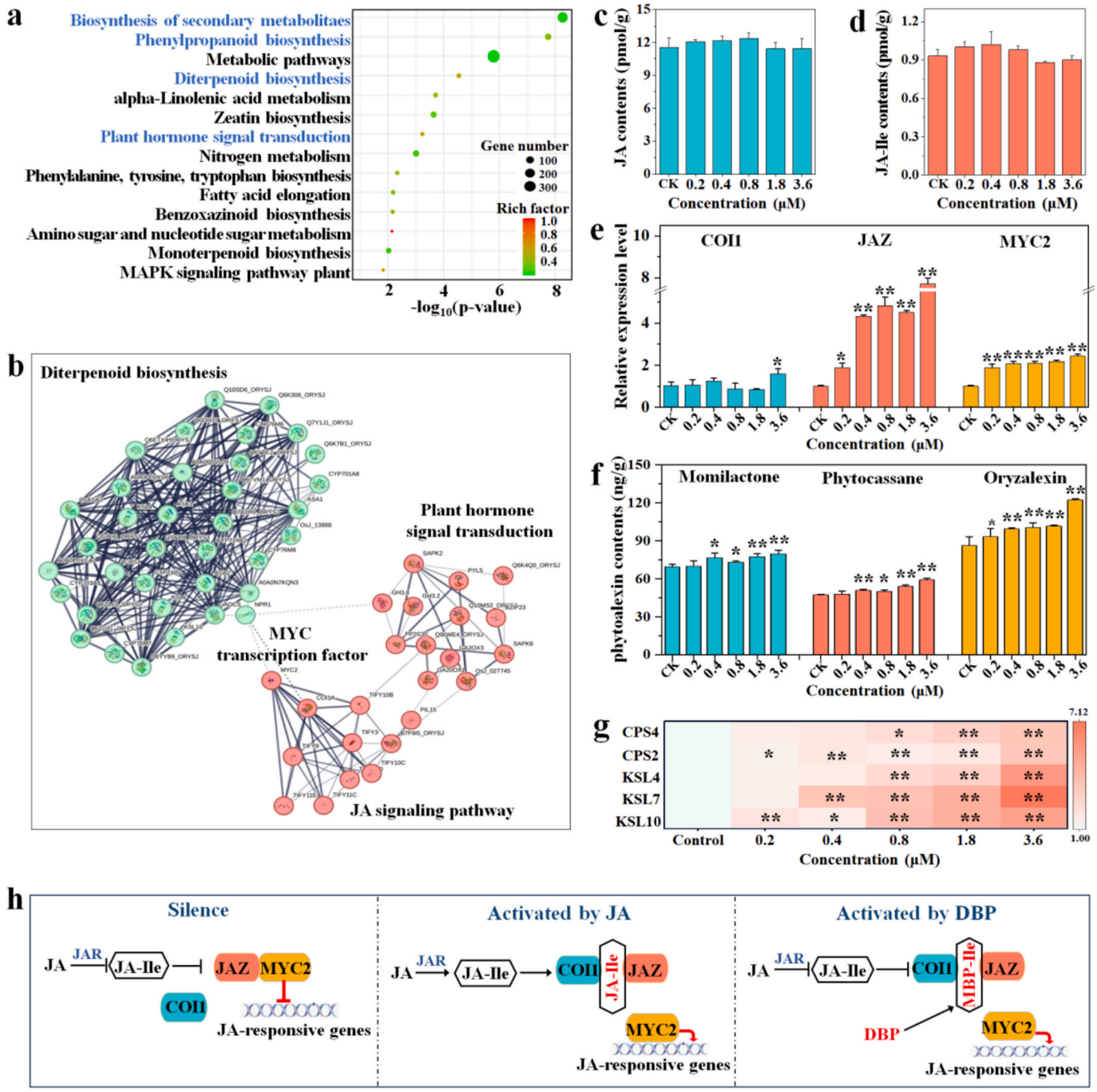

Fig. 2. The activation of the JA signaling pathway. (a) Metabolic pathway enrichment analysis in rice seedlings. Log10(p-value) represents the statistical test value (*t*-test) of the difference in gene expression level. (b) Protein − protein interaction network analysis of differentially expressed genes. (c) The content of JA. (d) The content of JA-Ile. (e) Gene expression encoding COI1, JAZ, and MYC2 in the JA signaling pathway. (f) Contents of phytoalexins include momilactones, phytocassanes, and oryzalexins. (g) Gene expression encoding key enzymes (i.e., CPS4, CPS2, KSL4, KSL7, and KSL10) responsible for the phytoalexins synthesis. (h) Schematic illustration of the non-essential activation of the biotic defense mechanisms in rice seedlings under DBP stress. CK: Control.

3.3. DBP transformation products activated JA signaling pathway

The chemical structure of a ligand determines its specificity in receptor-ligand recognition and structurally similar compounds may share a common molecular mechanism of action. One example supporting this stemmed from coronatine, a toxin produced by plant pathogenic strains of *Pseudomonas syringae*, could be recognized by the receptor (i,e., COI1-JAZ co-receptor complexes) in the JA signaling pathway due to the structural similarity with JA (Katsir et al., 2008; Fonseca et al., 2009). In this study, up to 10.8–20.6 % DBP (*m/z* 279.1576; $[M + H]^+$) was hydrolyzed to monobutyl phthalate (MBP) (*m/z* 223.0952, $[M + H]^+$) by substituting of an aliphatic chain in DBP with a carboxyl group to form acetate side chain (Table S3, Fig. S7 and Fig. 3b). Two common characteristic product ions originating from MBP (*m/z* 121.0271 and 149.0226) were observed. Similar conversion of PAEs have been documented in previous studies (Sun et al., 2015; Xing et al., 2023). Coincidentally, JA, a plant hormone, shares the substructure of an aliphatic chain and an acetate side chain with MBP. Furthermore, coupling with amino acids (e.g., isoleucine, Ile) was a prerequisite for the bioactivation and functionality of JA hormone, and

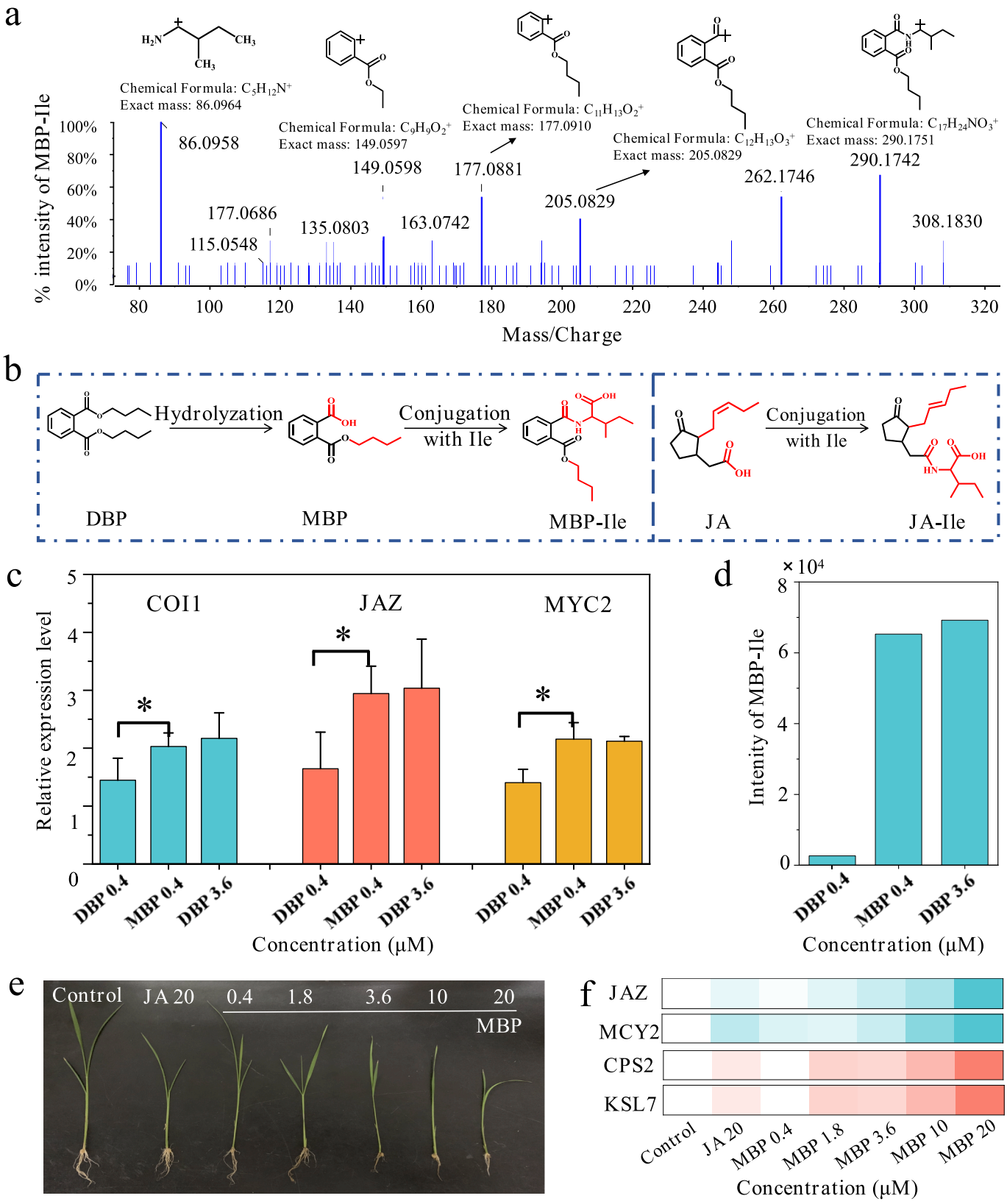

Fig. 3. DBP transformation metabolites activated the JA signaling pathway. (a) MS/MS spectrum of MBP-Ile conjugates. (b) Proposed biotransformation pathways from DBP to MBP-Ile. (c) Gene expression levels of COI1, JAZ, and MYC2 in the JA signaling pathway. (d) The signal intensity of MBP-Ile in rice leaves after treated with 0.4 μM DBP, 0.4 μM MBP, or 3.6 μM DBP. (e) The rice growth under MBP exposure with JA as positive control. (f) The JA related gene expression under MBP exposure with JA as positive control.

MBP-Ile conjugates (MS parameters: *m/z* 336.1784, $[M + H]^+$) were also identified in rice leaves (Fig. 3a and Fig. S8). Therein, the product ions *m/z* 86.0958 ($C_5H_{12}N^+$) matches the Ile-derived immonium ion, a hallmark of amino acid conjugation, *m/z* 205.0829 ($C_{12}H_{13}O_3^+$) corresponds to the core MBP after lossing Ile, and *m/z* 177.0881 ($C_{11}H_{13}O_2^+$) represents the core MBP after loss of the carboxyl group and Ile. This molecular ion aligns with the expected adduct structure, where MBP conjugates with Ile via an amide bond, followed by neutral loss of H_2O during ionization.

Considering the influence of Ile fluctuation on the formation of MBP-Ile in rice plants, we determined the isoleucine concentration in rice leaves of control group (without exposed to MBP) and the MBP exposed groups. Results showed that the Ile concentrations was ranged from 4.12 to 4.59 μmol/g under 0.2–3.6 μM MBP exposure, exhibited comparable to control group (4.57 μmol/g, $p > 0.05$) (Fig. S9). The concentration MBP in rice leaves were ranged from 1.23–1.87 nmol/g (0.33–0.50 μg/g) under 0.2–3.6 μM MBP exposure (Table S3), which is about 3000 times different from the Ile level, indicating that the MBP-Ile formation was driven by MBP availability rather than isoleucine level. Therefore, the interference of fluctuations in endogenous isoleucine levels to MBP-Ile formation might not be considered. The result tentatively confirmed our speculation that MBP would intervene in the JA signaling pathway and consequently triggering adverse corresponding outcomes in rice.

To distinguish the effects of MBP from DBP, rice seedlings were cultivated separately with each compound. Comparing the transcriptional level of genes under the stress of 0.4 μM of DBP or MBP, we found that the expression levels of COI1, JAZ, and MYC2 in the MBP group were 1.40, 1.53, and 1.53 folds of that in the DBP group, respectively, which were possibly attributed to the higher enriched concentration of MBP-Ile in rice leaves after a direct exposure to MBP (Fig. 3d). The *in vivo* concentration of the metabolite MBP detected in rice leaves exposed to 0.4 μM of DBP was ~10 % of the parent DBP (Table S3), thus we next conducted the comparative hydroponic experiment between 0.4 μM MBP and 3.6 μM DBP. It was observed that after 14-day cultivation, the expression of genes encoding COI1, JAZ, and MYC2 under the two exposures was significantly upregulated at comparable levels, with insignificant differences between them (Fig. 3c). Moreover, the peak intensities of MBP-Ile conjugate in the two groups were not significantly different as well (Fig. 3d). In addition, when compared the biomass inhibition effects on rice seedlings beween DBP and MBP, we found that MBP exposure caused significant dose-dependent reductions in rice biomass (22.3–37.6 %), which was stronger than DBP exposure (7.73–16.7 %) (Fig. S10). The result semiquantitatively suggested that the JA signal initiation and relevant phenotypic disturbance observed in DBP-exposed rice plants may be attributed by the MBP metabolite.

To elucidate the comparative effects of MBP and JA, we established a parallel experimental system incorporating 20 μM JA-treated rice seedlings as a positive control. As illustrated in Fig. S11, exposure to 0.4 μM MBP induced negligible alterations in rice height and starch content compared to the control group, likely due to the resistance nature of plants to adversity (Li et al., 2024). In contrast, MBP at 1.8–3.6 μM MBP significantly suppressed growth, reducing rice height and starch content by 19.7–26.3 % and 29.9–46.3 %, respectively. These inhibitory trends mirrored those observed under JA treatment at 20 μM, where rice height and starch content decreased by 23.6 % and 29.2 %, respectively. Transcriptomic analysis further revealed that MBP exposure at 0.4–20 μM significantly upregulated JAZ (by 1.20–4.60 folds) and MYC2 (by 1.81–5.40 folds) expressions in rice leaves. JA treatment at 20 μM similarly elevated JAZ (by 1.50 folds) and MYC2 (by 2.69 folds) expression. Additionally, downstream JA-responsive genes, including CPS2 and KSL7, were markedly induced by both JA (CPS2: 2.44 folds; KSL7: 2.59 folds) and MBP (CPS2: 3.89–8.93 folds; KSL7: 6.27–13.92 folds) exposures. These findings collectively demonstrated that MBP activated the JA signaling pathway in a manner analogous to endogenous JA. We further explored the interaction of MBP-Ile conjugate with the receptor proteins, aiming at clarifying the role and mechanism of MBP in JA signaling transduction.

3.4. The structural basis of MBP to participate in JA signaling pathway

Molecular docking simulation was employed to decipher the interaction mode between MBP-Ile and the COI1-JAZ co-receptor protein in rice, and homology modeling was applied to address the absence of a crystal structure for the COI1-JAZ co-receptor complexes in rice (Waterhouse et al., 2018; Liang et al., 2022; Zhang et al., 2018). It was shown that 96.6 % of amino residues in the COI1-JAZ complexes fall within acceptable regions of the Ramachandran plot, which exceeds the 90 % threshold in estimating the applicability of the model (Fig. S12) (Wan et al., 2017).

Following this, we embarked on docking MBP-Ile or JA-Ile with the COI1-JAZ complexes using Discovery Studio 2019. The result unveiled the spatial configuration of docking pockets for both MBP-Ile and JA-Ile to the COI1-JAZ complexes showcased almost perfect consistency (Fig. 4 and Fig. S13), indicating a comparable binding pattern between MBP-Ile and JA-Ile when engaged with COI1-JAZ complexes. Common interaction residues, such as ARG398, ARG337, TYR375, ARG573, ARG74, VAL400, ALA373, TRP508, and LEU458, which accounted for 82 % of the binding sites, underscored the shared interaction framework of MBP-Ile and JA-Ile to COI1-JAZ complexes. The interaction between JA-Ile and COI1-JAZ complexes was dominated by conventional hydrogen bonds, alkyl interactions, and salt bridges. Distinctively, the interaction of MBP-Ile was characterized by additional π–π stacking and an augmented number of salt bridges, enhancing its intermolecular interaction forces (Fig. S13). The phenyl ring in MBP-Ile facilitated a unique π–π stacking with PHE78, boosting the binding affinity to the COI1-JAZ receptor (Carter-Fenk et al., 2023). Salt bridges, representing a synergy of hydrogen and ionic bonds, outperform individual hydrogen bonds in binding energy (Choi et al., 2021), lending MBP-Ile an exceeded binding energy with COI1-JAZ complexes over JA-Ile (Fig. S13). These results provided a plausible explanation for why MBP-Ile, with a binding affinity of −395 kcal/mol with COI1-JAZ complexes, demonstrated a superior attachment to the receptor sites of JA-Ile, with −370 kcal/mol. It aligned with previous studies indicating xenobiotics resembling natural ligands, such as benzotriazole ultraviolet stabilizers and coronatine, can rival endogenous ligands for receptor sites, perturbing signal transduction processes (Katsir et al., 2008; Chen et al., 2023). The results signified the potential of MBP-Ile to disrupt the JA signaling pathway by competing for the COI1-JAZ receptor sites.

3.5. Extrapolation of toxicity mechanisms through a broader PAE spectrum

To examine the potential universality of JA-related toxicity among PAEs, four additional PAE congeners including dimethyl phthalate (DMP), diethyl phthalate (DEP), di-n-octyl phthalate (DnOP), diethylhexyl phthalate (DEHP), which were listed as priority pollutants by the US Environmental Protection Agency (USEPA), were selected to examine the adverse effects related to the JA signal pathway. First, we determined the transformed products of these chemicals in rice leaves. It was observed that they were hydrolyzed to MMP (*m/z* 181.0488, $[M + H]^+$), MEP (*m/z* 195.0650, $[M + H]^+$), MnOP (*m/z* 279.1574, $[M + H]^+$), and MEHP (*m/z* 279.1575, $[M + H]^+$), respectively (Fig. S14–S17). Moreover, while the contents of JA and JA-Ile exhibited no obvious change (Fig. S18), the gene expression levels of JAZ (3.4−6.8 folds) and MYC2 (2.0−3.2 folds) were significantly increased under DMP, DEP, DnOP, and DEHP exposures (Fig. 5a and Fig. S19). In addition, the downstream phytoalexin contents (i.e., momilactones, phytocassanes, and oryzalexins) and genes encoding their synthesis (i.e., CPS2, CPS4, KSL4, KSL7, and KSL10) were significantly up-regulated (Fig. 5b, Fig. S20, and Fig. S11). Consequently, the weights and lengths of rice roots, as well as the starch contents were significantly inhibited (Fig. S22).

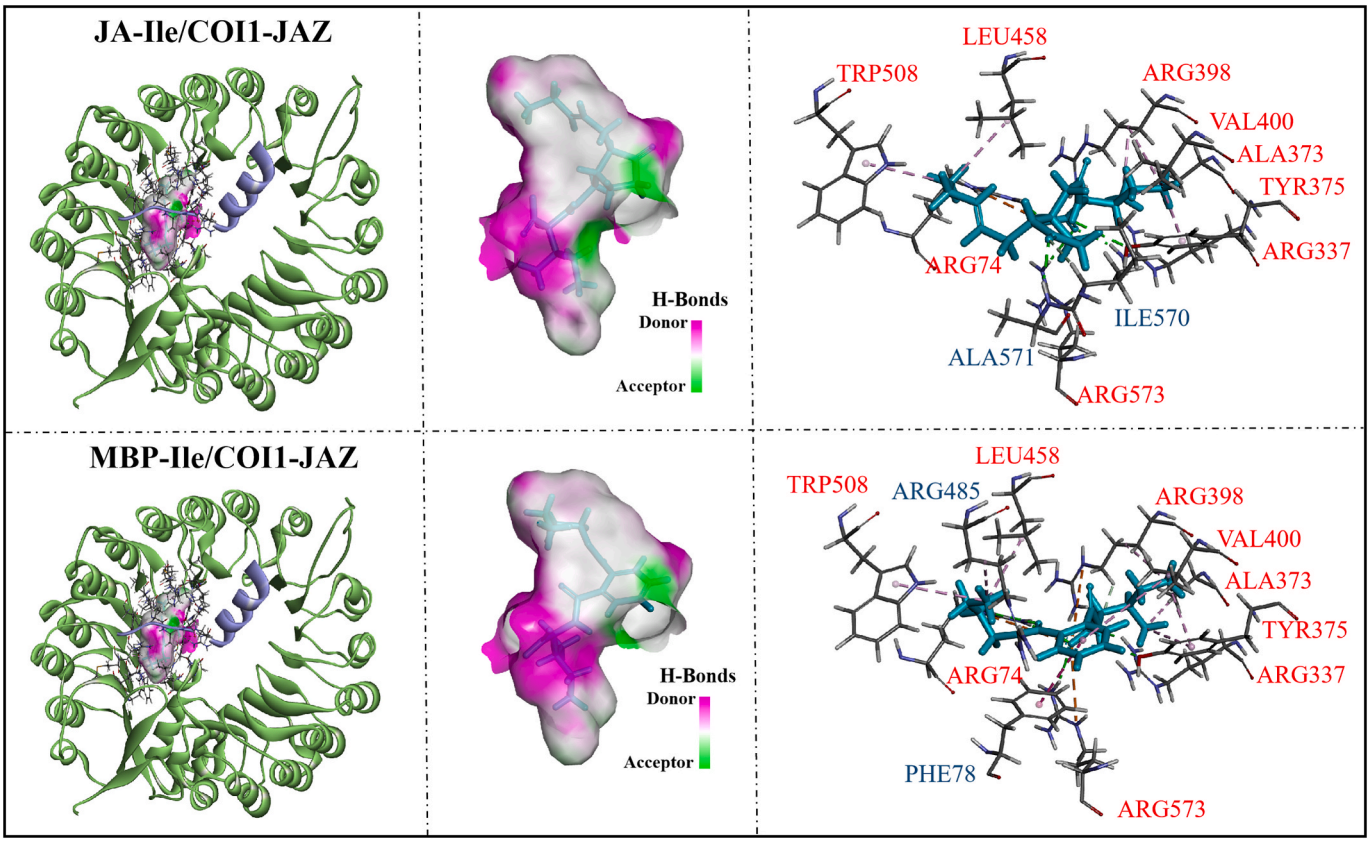

Fig. 4. Molecular docking simulations of JA-Ile and MBP-Ile with the COI1-JAZ co-receptor complex. The docking conformation, docking pocket, and 3D intermolecular interactions of interactions between JA-Ile, MBP-Ile, and COI1-JAZ co-receptor complex were shown in the left, middle, and right parts, respectively.

Furthermore, the molecular docking simulation was carried out to assess the binding modes of these four PAEs and the receptor protein, with JA-Ile as the positive control. The conformational superposition diagram displayed that the binding sites and docking pockets of MMP-Ile, MEP-Ile, MnOP-Ile, MEHP-Ile, and COI1-JAZ receptor complex were highly similar to those of JA-Ile. In addition, 73–91 % of the interaction residues of these couplers and COI1-JAZ were similar to JA-Ile, which provided a molecular interpretation for the observed JA-related toxicity (Fig. 5c and Fig. S23). Further correlating the ligand-receptor interaction with the adverse outcomes in rice plants, we found that the ranking of these binding energies aligned with the responses of the JA signaling pathway (Fig. 5d and Fig. S24). In detail, the binding energies ranked as MMP-Ile (−499 kcal/mol) > MEP-Ile (−461 kcal/mol) > MBP-Ile (−395 kcal/mol) > MnOP-Ile (−370 kcal/mol) > MEHP-Ile (−244 kcal/mol), which was significantly correlated with starch contents, phytoalexin contents, and gene expression of JAZ and MYC2 ($R^2 > 0.8$). The binding energies were also negatively correlated with the number of carbon atoms in the aliphatic chains of the selected PAE molecules ($R^2 = 0.84$, Fig. 5e). In summary, our study provided a mechanistic interpretation, from a structure-effect perspective, for the higher toxicity of the hydrolyzed products of PAEs (i.e., mPAEs) than the parents due to the role as JA structural analogues in plants.

4. Environmental implications

The widespread distribution and persistence of PAE contamination in agricultural soils have drawn considerable attention to crop yield and quality. PAEs were known to biotransform to more toxic metabolites after being uptake by crop. We discovered that MBP, the hydrolysis product of DBP, could mimic the function of JA and initiate the JA signaling pathway. The amino acid adduct of MBP (i.e., MBP-Ile) interacts with molecular switch proteins (i.e., COI1-JAZ co-receptor) of the JA signaling pathway, inducing an unintended defense response against herbivores through the synthesis of phytoalexins in rice. This enhanced pest defense was accompanied with reduced rice biomass and starch contents due to the reallocation of finite carbon resources from growth to defense. These findings were confirmed to be relevant using the other four PAEs. Overall, our work observed JA-related phonotypic disorders in rice exposed to PAEs and elucidated the mechanism regarding biotransformation and signaling transduction.

This toxic mechanism to PAEs was primarily linked to the JA-like hydrolysis products, which were characterized by the aliphatic chain and the acetate side chain. Some emerging alternatives of PAEs, such as diisononyl phthalate (DINP) and diisononyl hexahydrophthalate (DINCH), might also share a similar biotransformation and signaling pathway to inhibit crop growth. Focusing on the phytotoxicity mechanism of PAEs and their metabolites, our study opens a new viewpoint for the risk assessment and accurate design of PAE substitutes. Moreover, as a fundamental medium of plant growth, substantial areas of agricultural soil were covered with plastic mulching to conserve moisture. This practice inevitably results in an increased accumulation of PAEs in various edible crops, including wheat, maize, and vegetables. Therefore, the JA-signaling pathway-related disturbance under the PAE stress deserves in-depth and systematic investigation across diverse crop types.

While our current findings primarily focus on the rice seedling stage, chosen for its heightened sensitivity to pollutants and experimental controllability, we recognize that real-world agricultural scenarios involve chronic PAE exposure across all growth stages, with detectable residues persisting in edible tissues (Wu et al., 2023). Future research should expand to monitor JA signaling dynamics during critical developmental phases (tillering, flowering, and grain-filling), investigate environmental factors (e.g., soil properties and microbial activity), and validate findings through field studies comparing lab versus field responses. Given the evolutionary conservation of JA signaling across

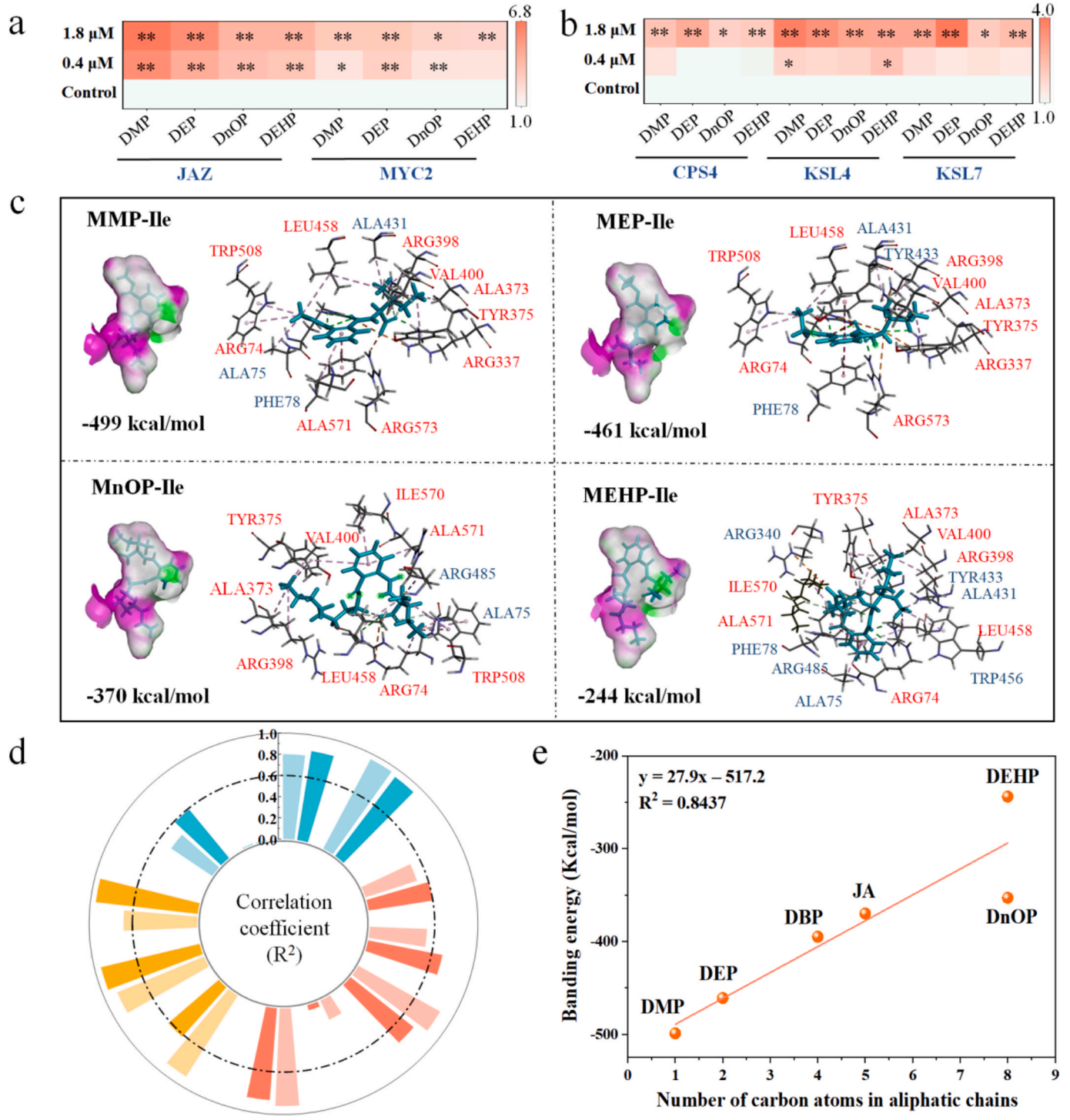

Fig. 5. The global changes in the JA signaling pathway exposed to DMP, DEP, DnOP, and DEHP. (a) The expression levels of key genes in the JA signaling pathway. (b) Gene expression encoding enzymes responsible for the phytoalexins synthesis. (c) Molecular docking results between DMP-Ile, DEP-Ile, DnOP-Ile, DEHP-Ile and the COI1-JAZ co-receptor. (d) The correlation coefficient between the binding energy and indicators of JA-related outcomes including phytoalexins contents (yellow columns), genes expression (blue-green columns), and growth indicators (red columns). Light and dark colors indicated the 0.4 and 1.8 μM group, respectively. (e) The correlation between carbon atom numbers in aliphatic chains and binding energy. (For interpretation of the references to color in this figure legend, the reader is referred to the web version of this article.)

plant species and the widespread detection of PAEs in various crops, we posit that this JA-mediated response mechanism likely operates under natural field conditions, warranting systematic investigation through well-designed field studies and multi-omics approaches to bridge laboratory findings with agricultural realities.

CRediT authorship contribution statement

Yingying Sun: Writing – original draft, Methodology, Data curation. **Jie Chen:** Writing – review & editing, Funding acquisition. **Wei Wang:** Writing – review & editing. **Lizhong Zhu:** Writing – review & editing, Project administration, Conceptualization.

Declaration of competing interest

The authors declare that they have no known competing financial interests or personal relationships that could have appeared to influence the work reported in this paper.

Acknowledgments

This work was supported by the National Natural Science Foundation of China (22436006 and 22306158).

Appendix A. Supplementary data

Supplementary data to this article can be found online at https://doi.org/10.1016/j.envint.2025.109553.

Data availability

Data will be made available on request.

References

Bertoft, E., 2017. Understanding starch structure: recent progress. Agronomy 7, 56.
Carter-Fenk, K., Liu, M., Pujal, L., Loipersberger, M., Tsanai, M., Vernon, R.M., Forman-Kay, J.D., Head-Gordon, M., Heidar-Zadeh, F., Head-Gordon, T., 2023. The energetic origins of pi–pi contacts in proteins. J. Am. Chem. Soc. 145, 24836–24851.
Chen, J., Wang, W., Chen, D.J., Zhu, L.Z., 2023. Benzotriazole ultraviolet stabilizers (BUVSs) as potential protein kinase antagonists in rice. Environ. Sci. Technol. 57, 21405–21415.
Chen, Y.M., Jin, G.C., Liu, M.Y., Wang, L.L., Lou, Y.G., Baldwin, I., Li, R., 2024. Multiomic analyses reveal key sectors of jasmonate-mediated defense responses in rice. Plant Cell 00, 1–16.
Cheng, Z.P., Sun, H.W., Sidhu, H.S., Sy, N.D., Gan, J., 2020. Metabolism of mono-(2-ethylhexyl) phthalate in Arabidopsis thaliana: Exploration of metabolic pathways by deuterium labeling. Environ. Pollut. 265, 114886.
Cheng, Z.P., Sun, H.W., Sidhu, H.S., Sy, N.D., Wang, X., Gan, J., 2021. Conjugation of di-n-butyl phthalate metabolites in arabidopsis thaliana and potential deconjugation in human microsomes. Environ. Sci. Technol. 55, 2381–2391.
Choi, M., Kim, J.G., Muniyappan, S., Kim, H., Kim, T.W., Lee, Y., Lee, S.J., Kim, S.O., Ihee, H., 2021. Effect of the abolition of intersubunit salt bridges on allosteric protein structural dynamics. Chem. Sci. 12, 8207–8217.
Deng, N.N., Grassini, P., Yang, H.S., Huang, J.L., Cassman, K.G., Peng, S.B., 2019. Closing yield gaps for rice self-sufficiency in China. Nat. Commun. 10, 1725.
Dueñas-Moreno, J., Mora, A., Cervantes-Avilés, P., Mahlknecht, J., 2022. Groundwater contamination pathways of phthalates and bisphenol A: origin, characteristics, transport, and fate – a review. Environ. Int. 170, 107550.
Fonseca, S., Chini, A., Hamberg, M., Adie, B., Porzel, A., Kramell, R., Miersch, O., Wasternack, C., Solano, R., 2009. (+)-7-iso-Jasmonoyl-L-isoleucine is the endogenous bioactive jasmonate. Nat. Chem. Biol. 5, 344–350.
Fu, W.J., Jin, G.C., Jiménez-Alemán, G.H., Wang, X.J., Song, J.X., Li, S.H., Lou, Y.G., Li, R., 2021. The jasmonic acid-amino acid conjugates JA-Val and JA-Leu are involved in rice resistance to herbivores. Plant Cell Environ. 45, 262–272.
Gao, M.L., Dong, Y.M., Zhang, Z., Song, W.H., Qi, Y., 2017. Growth and antioxidant defense responses of wheat seedlings to di-n-butyl phthalate and di (2-ethylhexyl) phthalate stress. Chemosphere 172, 418–428.
Gao, M.L., Xu, Y.L., Chang, X.P., Song, Z.G., 2021. Fe-Mn oxide modified biochar decreases phthalate uptake and improves grain quality of wheat grown in phthalate-contaminated fluvo-aquic soil. Chemosphere 270, 129428.
Guo, Q., Major, I.T., Howe, G.A., 2018. Resolution of growth–defense conflict: mechanistic insights from jasmonate signaling. Curr. Opin. Plant Biol. 44, 72–81.
Guo, W.L., Zhang, J.Y., Sun, Z.H., Orem, W.H., Tatu, C.A., Radulović, N.S., Milovanović, D., Pavlović, N.M., Chan, W., 2021. Analysis of polycyclic aromatic hydrocarbons and phthalate esters in soil and food grains from the balkan peninsula: implication on DNA adduct formation by aristolochic acid i and balkan endemic nephropathy. Environ. Sci. Technol. 55, 9024–9032.
Henkel, C., Hüffer, T., Hofmann, T., 2022. Polyvinyl chloride microplastics leach phthalates into the aquatic environment over decades. Environ. Sci. Technol. 56, 14507–14516.
Howe, G.A., Major, I.T., Koo, A.J., 2018. Modularity in jasmonate signaling for multistress resilience. Annu. Rev. Plant Biol. 69, 387–415.
Huot, B., Yao, J., Montgomery, B.L., He, S.Y., 2014. Growth–defense tradeoffs in plants: a balancing act to optimize fitness. Mol. Plant 7, 1267–1287.
Jiang, L.F., Zhu, X.P., Luo, C.L., Song, D.D., Song, M.K., 2022. The synergistic toxicity effect of di(2-ethylhexyl)phthalate and plant growth disturbs the structure and function of soil microbes in the rhizosphere. Environ. Int. 170, 107629.
Jiao, Y.Q., Tao, Y., Yang, Y., Diogene, T., Yu, H., He, Z.Q., Han, W., Chen, Z.B., Wu, P., Zhang, Y., 2020. Monobutyl phthalate (MBP) can dysregulate the antioxidant system and induce apoptosis of zebrafish liver. Environ. Pollut. 257, 113517.
Katsir, L., Schilmiller, A.L., Staswick, P.E., He, S.Y., Howe, G.A., 2008. COI1 is a critical component of a receptor for jasmonate and the bacterial virulence factor coronatine. Proc. Nat. Acad. Sci. 105, 7100–7105.
Kratochvil, I., Hofmann, T., Rother, S., Schlichting, R., Moretti, R., Scharnweber, D., Hintze, V., Escher, B.I., Meiler, J., Kalkhof, S., Bergen, M.V., 2019. Mono(2-ethylhexyl) phthalate (MEHP) and mono(2-ethyl-5oxohexyl) phthalate (MEOHP) but not di(2-ethylhexyl) phthalate (DEHP) bind productively to the peroxisome proliferatoractivated receptor γ. Rapid Commun. Mass Spectrom. 33, 75–85.
Le, T.M., Nguyen, H.M.N., Nguyen, V.K., Nguyen, A.V., Vu, N.D., Yen, N.T.H., Hoang, A. Q., Minh, T.B., Kannan, K., Tran, T.M., 2021. Profiles of phthalic acid esters (PAEs) in bottled water, tap water, lake water, and wastewater samples collected from Hanoi, Vietnam. Sci. Total Environ. 788, 147831.
Lee, Y.M., Lee, J.E., Choe, W., Kim, T., Lee, J.Y., Kho, Y., Choi, K., Zoh, K.D., 2019. Distribution of phthalate esters in air, water, sediments, and fish in the Asan Lake of Korea. Environ. Int. 126, 635–643.
Li, C., Xu, M.X., Cai, X., Han, Z.G., Si, J.P., Chen, D.H., 2022. Jasmonate signaling pathway modulates plant defense, growth, and their trade-offs. Int. J. Mol. Sci. 23, 3945.
Li, K., Ma, D., Wu, J., Chai, C., Shi, Y., 2016. Distribution of phthalate esters in agricultural soil with plastic film mulching in Shandong Peninsula, East China. Chemosphere 164, 314–321.
Li, R., Jin, J.J., Xu, J., Wang, L.L., Li, J.C., Lou, Y.G., Baldwin, I.T., 2020. Long non-coding RNAs associate with jasmonate-mediated plant defence against herbivores. Plant Cell Environ. 44, 982–994.
Li, X.C., Schuler, M.A., Berenbaum, M.R., 2002. Jasmonate and salicylate induce expression of herbivore cytochrome P450 genes. Nature 419, 712–715.
Li, Y., Zhang, K., Chen, J., Zhang, L., Feng, F., Cheng, J., Ma, L., Li, M., Wang, Y., Jiang, W., Yu, X., 2024. Rhizosphere Bacteria Help to Compensate for Pesticide-Induced Stress in Plants. Environ. Sci. Technol. 58, 12542–12553.
Liang, J.F., Ji, X.M., Feng, X.X., Su, P.J., Xu, W.Z., Zhang, Q.Z., Ren, Z.H., Li, Y.L., Zhu, Q. Q., Qu, G.B., Liu, R.Z., 2024. Phthalate acid esters: A review of aquatic environmental occurrence and their interactions with plants. J. Hazard. Mater. 470, 134187.
Liang, X.S., Zhang, H., Wang, Z.Y., Zhang, X., Dai, Z.Y., Zhang, J., Luo, P., Zhang, L.B., Hu, J., Liu, Z.Q., Bi, C.L., Cheng, Q., 2022. JMJD8 is an M2 macrophage biomarker, and it associates with DNA damage repair to facilitate stemness maintenance, chemoresistance, and immunosuppression in pan-cancer. Front. Immunol. 13, 875786.
Ma, T., Zhou, Y., Xia, Y.H., Meng, X.N., Jin, H.B., Wang, B., Chen, Y.S., Qiu, J.Y., Wu, J., Ding, J., Han, X.D., Li, D.M., 2020. Maternal exposure to di-n-butyl phthalate promotes the formation of testicular tight junctions through downregulation of NF-κB/COX-2/PGE2/MMP-2 in mouse offspring. Environ. Sci. Technol. 54, 8245–8258.
Machado, R.A.R., Ferrieri, A.P., Robert, C.A.M., Glauser, G., Kallenbach, M., Baldwin, I. T., Erb, M., 2013. Leaf-herbivore attack reduces carbon reserves and regrowth from the roots via jasmonate and auxin signaling. New Phytol. 200, 1234–1246.
Montea, I., Caballerob, J., Zamarreñoc, A.M., Fernández-Barberoa, G., García-Minac, J. M., Solanoa, R., 2022. JAZ is essential for ligand specificity of the COI1/JAZ co-receptor. Proc. Nat. Acad. Sci. 119, e2212155119.
Net, S., Sempéré, R., Delmont, A., Paluselli, A., Ouddane, B., 2015. Occurrence, fate, behavior and ecotoxicological state of phthalates in different environmental matrices. Environ. Sci. Technol. 49, 4019–4035.
Nguyen, L.V., Diamond, M.L., Kalenge, S., Kirkham, T.L., Holness, D.L., Arrandale, V.H., 2022a. Occupational exposure of canadian nail salon workers to plasticizers including phthalates and organophosphate esters. Environ. Sci. Technol. 56, 3193–3203.
Nguyen, T.G., Goossens, A., Lacchini, E., 2022b. Jasmonate: A hormone of primary importance for plant metabolism. Curr. Opin. Plant Biol. 67, 102197.
Niu, L.L., Xu, Y., Xu, C., Yun, L., Liu, W.P., 2014. Status of phthalate esters contamination in agricultural soils across China and associated health risks. Environ Pollut. 195, 16–23.
Sheard, L.B., Tan, X., Mao, H., Withers, J., Ben-Nissan, G., Hinds, T.R., Kobayashi, Y., Hsu, F.F., Sharon, M., Browse, J., He, S.Y., Rizo, J., Howe, G.A., Zheng, N., 2010. Jasmonate perception by inositol-phosphate-potentiated COI1–JAZ co-receptor. Nature 468, 400–405.
Shi, W., Zhang, F.X., Hu, G.J., Hao, Y.Q., Zhang, X.W., Liu, H.L., Wei, S., Wang, X.R., Giesy, J.P., Yu, H.X., 2012. Thyroid hormone disrupting activities associated with phthalate esters in water sources from Yangtze River Delta. Environ. Int. 42, 117–123.
Shinohara, N., Oguri, T., Takagi, M., Ueyama, J., Isobe, T., 2024. Evaluating the risk of phthalate and non-phthalate plasticizers in dust samples from 100 Japanese houses. Environ. Int. 183, 108399.
Staswick, P.E., Tiryaki, I., 2004. The oxylipin signal jasmonic acid is activated by an enzyme that conjugates it to isoleucine in arabidopsis. Plant Cell 16, 2117–2127.
Sun, B.R., Li, W.L., Ma, Y.M., Yu, T., Huang, W.J., Ding, J.R., Yu, H., Jiang, L.Q., Zhang, J., Lv, S.W., 2023. OsGLP3-7 positively regulates rice immune response by activating hydrogen peroxide, jasmonic acid, and phytoalexin metabolic pathways. Mol. Plant Pathol. 24, 248–261.
Sun, J.T., Wu, X., Gan, J., 2015. Uptake and metabolism of phthalate esters by edible plants. Environ. Sci. Technol. 49, 8471–8478.
Takaoka, Y., Iwahashi, M., Chini, A., Saito, H., Ishimaru, Y., Egoshi, S., Kato, N., Tanaka, M., Bashir, K., Seki, M., Solano, R., Ueda, M., 2018. A rationally designed JAZ subtype-selective agonist of jasmonate perception. Nat. Commun. 9, 3654.
Thines, B., Katsir, L., Melotto, M., Niu, Y., Mandaokar, A., Liu, G.H., Nomura, K., He, S. Y., Howe, G.A., Browse, J., 2007. JAZ repressor proteins are targets of the SCF^{COI1} complex during jasmonate signalling. Nature 448, 661–665.

Wan, W.N., Huang, H.L., Lv, J.T., Han, R.X., Zhang, S.Z., 2017. Uptake, translocation, and biotransformation of organophosphorus esters in wheat (*Triticum aestivum L.*). Environ. Sci. Technol. 51, 13649–13658.

Wang, W., Kannan, K., 2023. Leaching of phthalates from medical supplies and their implications for exposure. Environ. Sci. Technol. 57, 7675–7683.

Wang, L.L., Xua, G.J., Li, L.H., Ruan, M.Y., Bennion, A., Wang, G.L., Li, R., Qu, S.H., 2023. The OsBDR1-MPK3 module negatively regulates blast resistance by suppressing the jasmonate signaling and terpenoid biosynthesis pathway. Proc. Nat. Acad. Sci. 120, e2211102120.

Wang, Y., Wang, F., Xiang, L.L., Gu, C.G., Redmile-Gordon, M., Sheng, H.J., Wang, Z.Q., Fu, Y.H., Bian, Y.R., Jiang, X., 2021. Risk assessment of agricultural plastic films based on release kinetics of phthalate acid esters. Environ. Sci. Technol. 55, 3676–3685.

Wang, Y., Deng, C., Elmer, W.H., Dimkpa, C.O., Sharma, S., Navarro, G., Wang, Z., LaReau, J., Steven, B.T., Wang, Z., Zhao, L., Li, C., Dhankher, O.P., Gardea-Torresdey, J.L., Xing, B., White, J.C., 2022. Therapeutic delivery of nanoscale sulfur to suppress disease in tomatoes: *In vitro* imaging and orthogonal mechanistic investigation. ACS Nano 16 (7), 11204–11217.

Waterhouse, A., Bertoni, M., Bienert, S., Studer, G., Tauriello, G., Gumienny, R., Heer, F. T., de Beer, T.A.P., Rempfer, C., Bordoli, L., Lepore, R., Schwede, T., 2018. SWISS-MODEL: homology modelling of protein structures and complexes. Nucleic Acids Res. 46, W296–W303.

Weng, X.Y., Zhu, Q.Q., Liao, C.Y., Jiang, G.B., 2023. Cumulative exposure to phthalates and their alternatives and associated female reproductive health: body burdens, adverse outcomes, and underlying mechanisms. Environ. Sci. Technol. 57, 8189–8212.

Wu, J., Lai, Y., Zhu, H., Yang, X., Ye, X., Zhang, A., Sun, J., 2023. Phthalate esters and their metabolites in paired soil-crop systems from farmland in major provinces of eastern China: Pollution characteristics and implications for human exposure. Sci. Total Environ. 882, 163645.

Wu, W., Hu, J., Wang, J.Q., Chen, X.R., Yao, N., Tao, J., Zhou, Y.K., 2015. Analysis of phthalate esters in soils near an electronics manufacturing facility and from a non-industrialized area by gas purge microsyringe extraction and gas chromatography. Sci. Total Environ. 508, 445–451.

Xing, H.H., Yu, X.L., Sun, J.T., Lu, G.N., Zhu, M.H., Liang, J.H., Jin, L., Zhu, L.Z., 2023. Interaction between phthalate ester and rice plants: novel transformation pathways and metabolic-network perturbations. Environ. Sci. Technol. 57, 8870–8882.

Zander, M., Lewsey, M.G., Clark, N.M., Yin, L., Bartlett, A., Saldierna Guzmán, J.P., Hann, E., Langford, A.E., Jow, B., Wise, A., Nery, J.R., Chen, H., Bar-Joseph, Z., Walley, J.W., Solano, R., Ecker, J.R., 2020. Integrated multi-omics framework of the plant response to jasmonic acid. Nat. Plants 6, 290–302.

Zhang, Q.Q., Ma, Z.R., Cai, Y.Y., Li, H.R., Ying, G.G., 2021. Agricultural plastic pollution in china: generation of plastic debris and emission of phthalic acid esters from agricultural films. Environ. Sci. Technol. 55, 12459–12470.

Zhou, Q., Wang, J.J., Meng, B.D., Cheng, J.Q., Lin, G.P., Chen, J.C., Zheng, D., Yu, Y.H., 2013. Distribution and sources of organochlorine pesticides in agricultural soils from central China. Ecotox. Environ. Safety 93, 163–170.

Kah, M., Tufenkji, N., White, J.C., 2019. Nano-enabled strategies to enhance crop nutrition and protection. Nat. Nanotechnol. 14, 532–540.

Zhang, Q., Ji, S.J., Chai, L.H., Yang, F.X., Zhao, M.R., Liu, W.P., Schüürmann, G., Ji, L., 2018. Metabolic mechanism of aryl phosphorus flame retardants by cytochromes P450: a combined experimental and computational 5. Study on triphenyl phosphate. Environ. Sci. Technol. 52, 14411–14421.

Zhu, T.K., Du, P.P., Zeng, L.J., Lu, H., Zhao, H.M., Li, Y.W., Mo, C.H., Cai, Q.Y., 2019. Variation in metabolism and degradation of di-n-butyl phthalate (DBP) by high- and low-DBP accumulating cultivars of rice (*Oryza sativa L.*) and crude enzyme extracts. Sci. Total Environ. 668, 1117–1127.

Zhuang, Y.Q., Wang, X.J., Llorca, L.C., Lu, J., Lou, Y.G., Li, R., 2021. Role of jasmonate signaling in rice resistance to the leaf folder *Cnaphalocrocis medinalis*. Plant Mol. Biol. 109, 627–637.